References

[1] K. Chang *et al.*, "High power 94 GHz pulsed IMPATT Oscillators," in *1979 IEEE-MTT-S Microwave Symp. Dig. Tech. Papers,* pp. 72–72, May 1979.

[2] H. J. Kuno and D. L. English, "Millimeter-wave IMPATT power amplifier/combiner," *IEEE Trans. Microwave Theory Tech.,* vol. MTT-24, pp. 758–767, Nov. 1976.

[3] C. T. Rucker, "A multiple-diode high-average-power avalanche diode oscillator," *IEEE Trans. Microwave Theory Tech.,* vol. MTT-17, pp. 553–555, Dec. 1969.

[4] J. P. Quine, J. G. McMullen, and D. D. Khandelwal, "*Ku*-Band IMPATT amplifiers and power combiners," in *1978 IEEE-MIT Microwave Symp. Dig. Tech. Papers,* pp. 346–348, June 1978.

[5] E. J. Wilkinson, "An *N*-way hybrid power divider," *IRE Trans. Microwave Theory Tech.,* vol. MTT-8, pp. 116–118, Jan. 1960.

[6] K. Kurokawa and F. M. Magalhaes, "An *X*-band 10-watt multiple-IMPATT oscillator," *Proc. IEEE,* vol. 59, pp. 102–103, Jan. 1971.

[7] R. S. Harp and H. L. Stover, "Power combining of *X*-band IMPATT circuit modules," in *1973 IEEE-ISSCC Dig. Tech. Papers,* vol. XVI, pp. 118–119, Feb. 1973.

[8] R. N. Wallace, M. G. Adlerstein, and S. R. Steele, "A 60-W CW solid-state oscillator at *C*-band," *IEEE Trans. Microwave Theory Tech.,* vol. MTT-24, pp. 483–485, July 1976.

[9] F. J. Bayuk and J. E. Raue, "*Ka*-band solid state power combiner," in *1977 IEEE Microwave Symp. Dig. Tech. Papers,* pp. 29–31, June 1977.

[10] M. Dydyk, "Efficient power combining," in *1979 IEEE Microwave Symp. Dig. Tech. Papers,* pp. 309–310, May 1979.

[11] G. L. Ragan, *Microwave Transmission Circuits,* vol. 9 (MIT Radiation Lab. Series). New York: McGraw-Hill, 1948.

[12] N. D. Kenyon, "A circuit design for *MM*-wave IMPATT oscillators," in *1970 IEEE-MIT Microwave Symp. Dig. Tech. Papers,* pp. 300–303, May 1970.

[13] F. M. Magalhaes and K. Kurkowa, "A single-tuned oscillator for IMPATT characterization," *Proc. IEEE* (Lett.), vol. 58, pp. 831–832, May 1970.

[14] L. Lewin, "A contribution to the theory of probes in waveguides," *Proc. Inst. Elec. Eng.,* Monogr. 259R, pp. 109–116, Oct. 1957.

[15] ——, *Theory of Waveguides.* New York: Wiley 1975, Ch. 5.

[16] R. L. Eisenhart *et al.,* "A useful equivalence for a coaxial-waveguide junction," *IEEE Trans. Microwave Theory Tech.,* vol. MTT-26, pp. 172–174, Mar. 1978.

[17] R. L. Eisenhart and P. J. Khan, "Theoretical and experimental analysis of a waveguide mounting structure," *IEEE Trans. Microwave theory tech.,* vol. MTT-19 pp. 706–719, Aug. 1971.

[18] R. L. Eisenhart, "Discussion of a 2-gap waveguide mount," *IEEE Trans. Microwave Theory Tech.,* vol. MTT-24, pp. 987–990, Dec. 1976.

[19] M. Marcuvitz, *Waveguide Handbook.* New York: McGraw-Hill, 1951.

[20] T. Misawa, "Negative resistance in p-n junction under avalanche breakdown conditions, Pts. I and II," *IEEE Trans. Electron Devices,* vol. ED-13, pp. 137–151, Jan. 1966.

[21] T. T. Fong, K. P. Weller, and D. L. English, "Circuit Characterization of *V*-band IMPATT oscillators and amplifiers," *IEEE Trans. Microwave Theory Tech.,* vol. MTT-24, pp. 752–758, Nov. 1976.

[22] G. L. Matthaei, L. Young, and E. M. T. Jones, *Microwave Filters, Impedance-Matching Networks and Coupling Structures.* New York: McGraw-Hill, 1964.

[23] K. Chang, R. Ebert, and C. Sun, "*W*-band two-diode power combiner," *Electron. Lett.,* vol. 15, no. 13, pp. 403–405, June 21, 1979.

Study of the Harmonic Effects for Waveguide Gunn-Diode Oscillator Optimization

EZIO M. BASTIDA, MEMBER, IEEE

***Abstract*—The dependence on harmonic load conditions of waveguide Gunn oscillator performance is theoretically and experimentally studied. A simple waveguide mount is presented, which by controlling the diode harmonic load conditions, with one single adjustment permits considerable simultaneous improvement in output power, bias tuning, and varactor tuning linearities, as well as in frequency stability with the temperature. The oscillator noise level can also be minimized, though not at the same time as the other improvements. Finally, the usefulness of harmonic control in simplifying some typical thermal procedures is shown.**

I. Introduction

FOR SOME YEARS waveguide Gunn-diode oscillators have played an important role as tunable microwave sources. This is due not only to their electrical properties but also to the fact that they can be very easily constructed. Their electromagnetic behavior, however, is remarkably complex and for this reason a great deal of attention has been devoted [1]–[5] to the synthesizing of oscillator equivalent circuits. The possibility of obtaining high power, efficient electronic tuning, a low FM noise level, and a good frequency stability with the temperature is, however, often affected by some nonlinear harmonic effects that are usually not considered in oscillator models. This work first presents a survey of the effects that limit oscillator power and FM–AFC performance. An analysis of the reasons for these limits allows us to bring out interesting properties of oscillator electronic tuning and to predict a nonnegligible effect of the diode harmonic load conditions on the oscillator frequency stability with temperature and on the FM noise level. Circuit requirements for overcoming the demonstrated limits are then discussed, and a Gunn-diode waveguide mounting that satisfies the requirements is described. Finally, experimental results obtained by using the mount are presented.

Manuscript received July 25, 1979; revised November 19, 1979.

The author is with the Centro Informazioni Studi Esperienze, CISE—P.O. Box 3986, 20100, Milano, Italy.

0018-9480/80/0400-0305$00.75 ©1980 IEEE

II. Phenomenological Description of the Effect of Harmonics on Oscillator Output Power and FM–AFC Characteristics

When the cavity size d of a post coupled oscillator (Fig. 1(a)) is varied sharp power fluctuations are often observed [6] which can be correlated by a parametric self-pumping mechanism—studied by Carrol [7] and other authors [8], [9]—with harmonic frequency long-line effects. Such undesired efficiency fluctuations and the very wide loaded Q variation with the cavity size d [10], make this very simple oscillator design rather impractical. A very smooth tuning is usually provided in iris-coupled oscillators (Fig. 1(b)). Sharp power fluctuations are then rarely observed and, owing to some decoupling due to the iris, they depend very slightly on the load. The output power level is, however, strongly affected by the harmonic frequency impedance seen by the diode.

The oscillator frequency f can be tuned (though only in very small bands) by changing the diode bias voltage V_d. This phenomenon was used to obtain frequency-modulated or automatic frequency controlled oscillators [11]–[13]. These systems have a drawback in that the bias-tuning sensitivity $\alpha = df/dV_d$ varies from one diode to another, while depending for the same diode on the circuit Q factor at the operating frequency [12]–[14]. Moreover, the α value depends on the load conditions at the harmonic frequencies and marked α fluctuations may also occur if the oscillator is connected to a very strongly harmonic reflecting load [15]. Output power level also depends on the harmonic load and the power–voltage curves ($P-V_d$) show an irregular trend, when the $\alpha(V_d)$ values also fluctuate. We systematically analyzed the ($f-V_d$) and ($P-V_d$) curves of an iris-coupled oscillator connected, at different distances d', to a harmonic reflecting filter (HP-X-362A). We observed marked nonlinearities in both types of diagrams but, choosing the proper distance d', it is always possible to obtain a flat $\alpha(V_d)$ trend and a smooth $P-V_d$ curve with a very high power level. Similar behavior was observed using a post coupled oscillator. Finally, we should point out that in varactor-tuned oscillators the frequency–varactor voltage ($f-V_v$) and the power–varactor voltage ($P-V_v$) curves exhibit a fluctuating trend very similar to the one described here for bias-tuning. Experimental results given in the final part of this work document this situation which holds true for both parallel-type (Fig. 1(c)) and series-type varactor mountings.

III. Analysis of Harmonic Effects on Oscillator Performance and Description of Circuit Requirements for Practical Optimization

The previous section shows the limits of waveguide Gunn-diode oscillator performance. The power level may be much lower than that the diode could supply. When the oscillator is frequency modulated, undesirable amplitude modulation may occur. The distortion of frequency–voltage plots limits FM performance and when it produces a variation of the df/dV sign compromises the

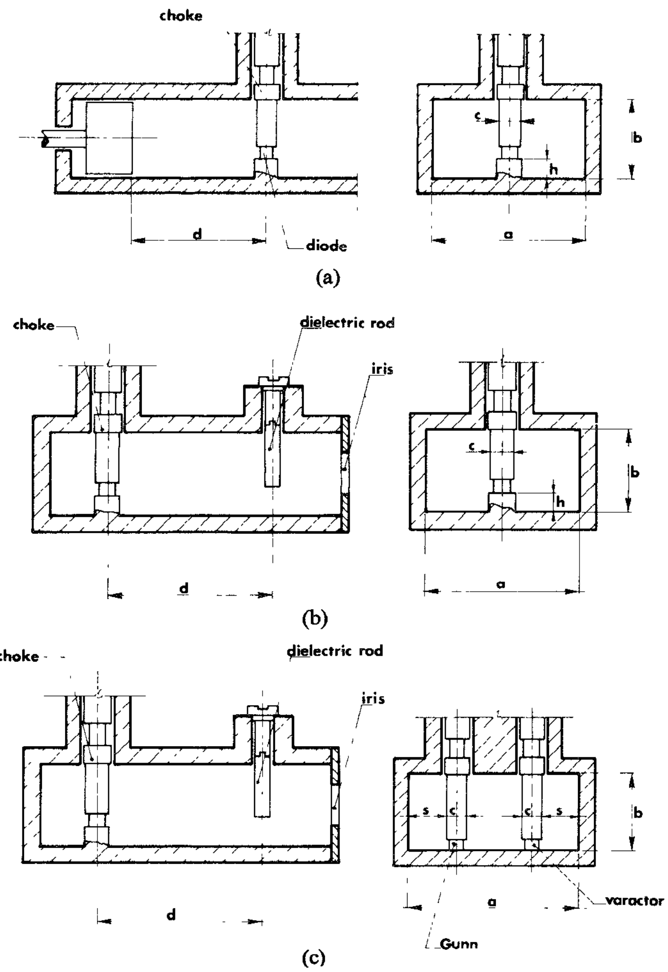

Fig. 1. (a) Full-height waveguide-tunable Gunn diode oscillators: Plunger mounting. (b) Iris and dielectric screw mounting. (c) A parallel type varactor mounting.

automatic frequency control capability. Since these effects strongly depend on the second harmonic load [6], [15], it is important to design a mount in which both the level and the trend of the second harmonic impedance seen by the diode can be widely varied without affecting the load conditions at the fundamental frequency, which can thus be independently optimized. Such a structure should also ensure considerable improvement in FM noise and in frequency stability with the temperature.

To demonstrate this statement and clarify the mechanisms mentioned, further analysis of the link between frequency pulling effects and oscillator harmonic load conditions is required. In this connection, there is a useful work by Quine [16] who found that for an oscillator using a two terminal negative resistance element the following resonance condition must be fulfilled:

$$\sum_{n=1}^{\infty} n|E_n|^2 B_n = 0 \qquad (1)$$

where E_n is the voltage nth harmonic applied to the diode and B_n is the total circuit susceptance at this harmonic. The assumption is made that in steady-state the $I(t)$ and $V(t)$ coordinates point describes zero-area cycles in the

$I-V$ plane. This assumption does not hold completely true for Gunn-diode oscillators, as was shown by Tsai and Rosenbaum [12] and was experimentally confirmed by the low-frequency Gunn-diode $I-V$ characteristics [17], and as we also ascertained for microwave diodes by using a general computer program, calculating the current and electric field profile in a Gunn diode operating into a linear circuit [18]. As was shown in another study [19], we too observed a marked dependence of these cycle areas on the amplitude of the oscillator signal.

Despite this situation, several authors [16], [20], [21] agree on the essential likelihood of the conclusions to be drawn from (1) concerning frequency pulling effects in Gunn-diode oscillators. It should also be noted that Wu [20] obtained experimental results supporting the reliability of (1).

As a first example, let us consider a diode coupled to a hypothetical cavity [16] formed by the parallel capacitance C (including the diode capacitance) and inductance L_n which is supposed to differ from one harmonic to another. Taking $f_{0n}=1/(2\pi\sqrt{L_nC})$, the circuit susceptance B_n at the nth harmonic of the operating frequency is given by

$$B_n(nf)=2\pi Cf_{0n}\left(\frac{nf}{f_{0n}}-\frac{f_{0n}}{nf}\right). \tag{2}$$

If we let $\delta f_n=nf-f_{0n}$ and if we suppose that, $|\delta f_n|/f_{0n}\ll 1$, from (1) and (2) we obtain:

$$\delta f_1=-\sum_{n=2}^{\infty} n|E_n/E_1|^2\delta f_n \tag{3}$$

where the δf_n cannot have all the same sign of δf_1 in order to satisfy the oscillation condition with $E_n\neq 0$. Let us now suppose that, by acting on capacitance C, we pass from the operating frequency f_α to the frequency $f_\beta=f_\alpha+\delta f$. If we let $\delta f_0=f_{01\beta}-f_{01\alpha}$, it is easy to find

$$\delta f=\delta f_0\frac{1+\sum_{n=2}^{\infty} n(f_{0n}/f_{01})|E_n/E_1|_\alpha^2}{1+\sum_{n=2}^{\infty} n^2|E_n/E_1|_\alpha^2} - \frac{\sum_{n=2}^{\infty} n\left(|E_n/E_1|_\beta^2-|E_n/E_1|_\alpha^2\right)\delta f_{n\beta}}{1+\sum_{n=2}^{\infty} n^2|E_n/E_1|_\alpha^2} \tag{4}$$

where indices α and β indicate the values assumed, respectively, by the various parameters in the initial and final condition.

The first term on the right in (4) gives the frequency variation when the diode voltage signal does not change its spectrum shape. A weak dependence of the oscillator frequency variations on the load conditions at harmonic frequencies is shown here ($\delta f<\delta f_0$ for inductive susceptance at all harmonics and $\delta f>\delta f_0$ for capacitive susceptance). However, the value of this term in any case is very close to δf_0. This can be easily verified by assuming that only the first two voltage harmonics are present. (We should point out in this connection that for waveguide Gunn-diode circuits, relative pulling effects $\delta f_1/f$ usually lower than 10^{-2} are observed, which is practically impossible to observe in computer simulations [18].) If we suppose for example that $\delta f_1/f=2\cdot 10^{-3}$ and $|E_2/E_1|=0.1$, then from (3) $f_{02}/f=f_{02}/f_{01}=2.1$ so that the first term on the right in (4) is equal to $1.002\delta f_0$. The fluctuations in tuning sensitivity are thus due to essential modifications of the signal spectrum shape and can really be observed only for small variations in the tuning itself.

This explains why for mechanical tuning, which often covers various gigahertz bands, no irregularities in tuning curves are usually observed [6]. The second term on the right in (4) (which is a nonlinear term as it depends on δf itself) shows that for harmonics that are all capacitively loaded ($\delta f_n>0$, $n\geq 2$), a reduction in tuning sensitivity is obtained when, as the frequency decreases ($\delta f, \delta f_0<0$), the harmonic content of the diode voltage spectrum is reduced. In this case the sign of the second term on the right in (4) is the opposite of that of δf_0. The contrary occurs when the diode is inductively loaded at the harmonics. Interesting experimental results reported by Pollmann and others [22] concerning a coaxial oscillator operating in parallel resonance conditions confirm the validity of (4) and show that load conditions minimizing the output power level ($P=P_{\min}$) are almost coincident with maximum frequency conditions ($f=f_{\max}$) while, vice-versa, optimal output power level conditions correspond to the frequency minimum. The same thing usually occurs in waveguide oscillators as well. In both conditions ($f_{\max}, P_{\min}$) and ($f_{\min}, P_{\max}$) high values of the $|E_2/E_1|$ ratio are measured [8], [24]. This observation allows us to show the possibility of simultaneously maximizing the output power and the temperature stability of an oscillator operating frequency which, as in our case, presents a negative derivative with temperature. This is due to the fact that as the temperature increases and frequency decreases, the relative harmonic content of the diode voltage signal usually also decreases. Reduction of the signal harmonic content is also observed when the computer program and circuits reported in [18] are used. The temperature dependence of the GaAs electron drift velocity reported in [23] was used for the computer simulation. The harmonic content reduction with increasing temperature is confirmed by Fig. 2(a) and (b), which show the $P-d$ curves at two different temperature values for a post coupled oscillator connected to a harmonic filter: at the higher temperature, a much lower relative amplitude of the power fluctuations is observed. In this connection, it is worth emphasizing, as pointed out by Kiehl and Gunshor [19], that small signal amplitudes facilitate the attainment of device linear dynamics.

As a second example, let us consider the case of a capacitance C_D (the diode capacitance) tuned in parallel by a series resonant circuit which is assumed to consist of a constant capacitance C, an inductance L_n, and a resistance R_n both differing from one harmonic to another.

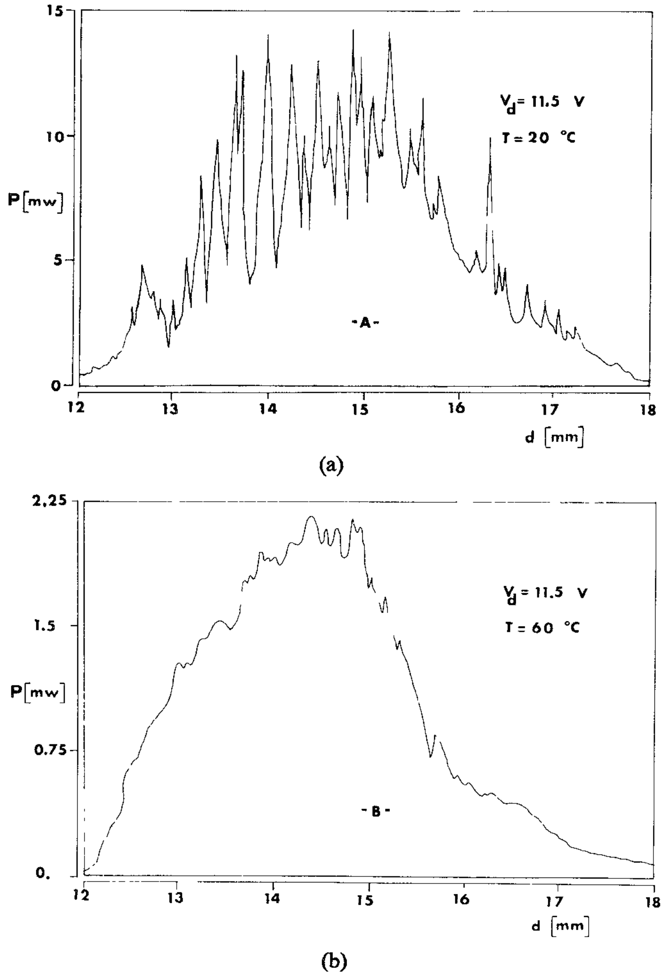

Fig. 2. Output power as a function of the position of the short-circuit plunger d for a post coupled X-band oscillator connected to a low-pass harmonic filter. The diagrams are for two different temperatures. (a) 20°C. (b) 60°C. The diode bias voltage was $V_d = 11.5$ V.

This model's greater possibilities for use with waveguide mountings as compared to the one described before, are made clear by Fig. 3, which shows the trend of the admittance seen by the semiconductor element at the fundamental frequency when the oscillator is connected directly with a matched load. In the calculations, made on the basis of the Eisenhart and Khan [24] model, it was assumed (Fig. 1(a)) that $c = 3.2$ mm and $d = 1.7$ cm and that the values of the case parasitic parameters were those reported in [25]. In Fig. 3 the line $-\omega C_D$ with $C_D = 0.2$ pF [26] is also traced. The intersection point A with the resonant circuit susceptance gives the oscillator operating point in the case of negligible harmonic effects. For this model, the B_n values to be introduced into the resonance condition (1) are given by

$$B_n = 2\pi n f C_D - \frac{\frac{Q_n}{R_n}\left(\frac{nf}{f_{0sn}} - \frac{f_{0sn}}{nf}\right)}{1 + Q_n^2\left(\frac{nf}{f_{0sn}} - \frac{f_{0sn}}{nf}\right)^2} \tag{5}$$

where f_{0sn} and Q_n are the resonant frequency and the Q factor at the nth harmonic of the series resonant circuit.

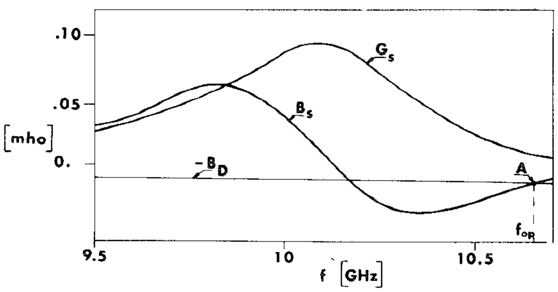

Fig. 3. Circuit admittance $Y_s = G_s + jB_s$ calculated for a distance $d = 1.7$ cm from the diode to the short circuit plunger. B_D is the diode susceptance calculated for a diode with 0.2-pF capacitance.

Now let us indicate by Δf the difference between the oscillator frequency f and the series circuit fundamental resonance frequency f_{0s1}. In the absence of harmonic effects $\left(\boldsymbol{a} = \sum_{n=2}^{\infty} B_n |E_n/E_1|^2 = 0\right)$, if we ignore the weak diode susceptance slope around the operating point, Δf is given by

$$\Delta f \cong f_{0s1} \frac{1 + \sqrt{1 + 4B_{0D}^2 R_1^2}}{4R_1 B_{0D} Q_1} \cong \frac{f_{0s1}}{2R_1 B_{0D} Q_1} \tag{6}$$

where it has been assumed (Fig. 3) that $4R_1^2 B_{0D}^2 \ll 1$, $\Delta f / f_{0s1} \ll 1$, and $B_{0D} = 2\pi f_{0s1} C_D$. For $\boldsymbol{a} \neq 0$, there is a further frequency variation δf_p so that

$$\delta f_p + \Delta f = f - f_{0s1} \cong \frac{f_{0s1}}{2R_1(B_{0D} + \boldsymbol{a})Q_1} = \frac{f_{0s1}}{2R_1 B_{0D} Q_{\text{eff}}} \tag{7}$$

where

$$Q_{\text{eff}} = \left(1 + \frac{\boldsymbol{a}}{B_{0D}}\right) Q_1 = \left(1 - \frac{B_1}{B_{0D}}\right) Q_1. \tag{7$'$}$$

This equation, where the relation $\boldsymbol{a} = -B_1$ taken from (1) has been used, describes the total frequency shift in terms of an equivalent Q factor of the series resonant circuit. Experimental data obtained, as described in [6], by varying only the impedance seen by the diode at the harmonic frequencies show $\delta f_p / f_{0s1}$ values in the $\pm 2.5 \cdot 10^{-3}$ range for a 10-GHz oscillator. Near the operating point the slope of the circuit susceptance is $dB/df = 0.1$ S/GHz: this corresponds for (7′) to a ± 20 percent Q_{eff} variation. When the admittance B_1 is strongly inductive (condition $f_{\min}, P_{\max}$) there is a maximum of Q_{eff}. On the contrary, a minimum is obtained for strongly capacitive B_1 (condition $f_{\max}, P_{\min}$). Let us now suppose we vary the Gunn-diode capacitance by δC_D. Indicating by $\delta \boldsymbol{a}$ the corresponding $\boldsymbol{a}$ variation, from (7) we obtain:

$$\delta f(\delta C_D) = -\frac{f_{0s1}}{2R_1 B_{0D} Q_{\text{eff}}} \left(\frac{\delta B_{0D} + \delta \boldsymbol{a}}{B_{0D} + \boldsymbol{a} + \delta B_{0D} + \delta \boldsymbol{a}}\right) \tag{8}$$

where

$$\delta B_{0D} = 2\pi f \delta C_D.$$

For a given variation of parameter $\boldsymbol{a}$ this relation allows us to predict a lower frequency sensitivity to the variations of the parameters affecting the diode equivalent capaci-

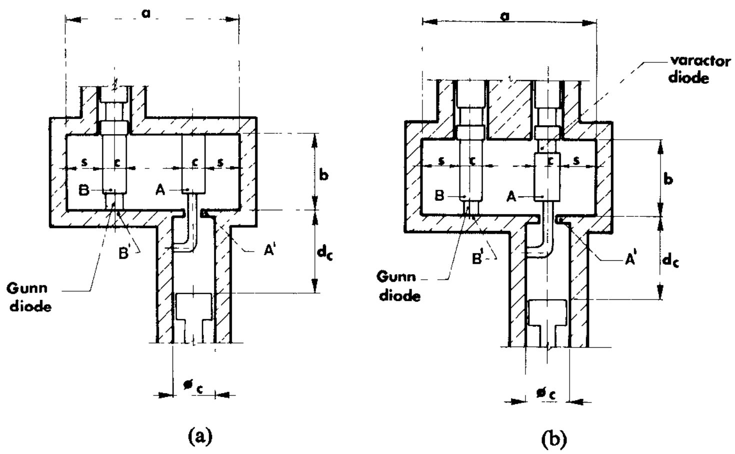

Fig. 4. The harmonic tuned mounting. (a) Without varactor. (b) With varactor.

tance (i.e., bias tuning, temperature effects, etc.) right at the condition $(f_{\min}, P_{\max})$ maximizing Q_{eff} and $(B_{0D}+a)$. It can also be seen that the frequency shift is fully compensated for when $\delta a = -\delta B_{0D}$. For diodes with negative temperature coefficients, δB_{0D} is positive for $\Delta T > 0$ and there is thus a compensating action for negative a variations. Under experimental conditions where the overall heating effect (including cavity expansion) is given, for any harmonic tuning condition, by a frequency decrease with temperature, this allows us to predict the minimum derivative at the condition $(f_{\min}, P_{\max})$, which makes the value a normally positive and maximum (in this connection it should be recalled that $a \to 0$ at high temperatures). Still using (8), it appears that the sensitivity of frequency variations to percentage variations of B_{0D} is lower for higher B_{0D} values. The result is a mechanism that brings about further stabilization at high temperatures and voltages, due to the fact that identical variations of a produce lower frequency shift effects as the diode temperature or voltage becomes higher. For very small variations of C_D, (8) can be written:

$$\delta f = -\frac{Q_1 f_{0s1}}{2R_1 B_{0D}^2 Q_{\text{eff}}^2}\left(1+\frac{\delta a}{\delta B_{0D}}\right)\delta B_{0D}. \qquad (8')$$

This relation is important for investigation of the harmonic effects on oscillator FM noise, which as is well known [27], is influenced to a remarkable extent by C_D fluctuations produced by diode bias voltage noise. Apparently the minimum noise condition requires that $\delta a/\delta B_{0D} = -1$; moreover at equal $\delta a/\delta B_{0D}$, the noise should be at a minimum precisely at the maximum Q_{eff} condition. The strong dependence on parameter $\delta a/\delta B_{0D}$ is however worth some further comment. In typical waveguide circuits, at equal variations of the tuning parameter (in our case B_{0D}), the impedance seen by the active element at the nth harmonic frequency exhibits many possible resonances, which increase rapidly with n [6]. Consequently, when the frequency is varied, rapid amplitude variations of very high frequency spectral components are generated. These components, whose intensity however is not such as to give easily detectable frequency pulling effects, strongly affect the value of $\delta a/\delta B_{0D}$ at the operating point. This may explain some results given in the last part of this work where it is shown that harmonic tuning may vary FM noise without remarkable changes in either oscillator frequency or power.

Finally, let us consider the effect of small variations in the tuning capacitance C of the series resonant circuit (think for example of thermal deformations of the resonant cavity or of varactor tuning). In this case the curve describing the resonant circuit susceptance shifts slightly, being deformed very little. As a result (dB_1/df) of the working point remains practically unvaried for constant a. Thus for this model as well, the effect of tuning parameter variations appears to be less important than that of signal spectral variations in the cavity. In this case for an increasing $C(\delta f_{0p}<0)$ there is a stabilizing effect at the condition $(f_{\min}, P_{\max})$ if a decreases.

IV. Mount with Mechanical Tuning at the Harmonic Frequencies

The schematic of the mount is shown in Fig. 4(a). It can be used in either iris-coupled or post-coupled configuration. The possibility of varying only the impedance seen by the semiconductor element at the harmonic frequencies (at the second one, to be precise, in particular) without directly affecting the impedance at the fundamental frequency is brought about through variation of the length d_c of a cylindrical cavity. This cavity, coupled with the circuit by a diodeless post, has a diameter such that the fundamental frequency component of the signal is cutoff. In the experimental tests reported herein we took $\phi = 12$ mm with a length d_c of the cylindrical cavity of not less than 10 cm in order to assure a drastic attenuation of the X-band fundamental frequency signal. Nevertheless, for cavities whose overall dimensions do not constitute a problem ($d_c \cong 2$ or 3 cm), behavior differing from that described was not observed. Since tuning at the harmonic frequencies gives rise to pulling effects $\delta f/f < 10^{-2}$, it was possible to draw the mechanical tuning curve. For a plunger-tuned post coupled configuration a band 4.5 GHz wide was obtained by varying the plunger distance d from the diode between 12 and 22 mm. Suppose we now connect the oscillator to a load that is purely reactive at the second harmonic (such as, for instance, the low-pass filter). In this case, by varying the cylindrical cavity short-circuit position d_c, a reactance jX_c ranging between $+j\infty$ and $-j\infty$ is seen at the input of the lossless two-port $(A-A')-(B-B')$ of Fig. 5. Thus, disregarding the case of total decoupling, a second harmonic reactance, also variable between $-j\infty$ and $+j\infty$, is brought back through the two-port $(A-A')-(B-B')$ to $(B-B')$ and from there directly to the semiconductor. In this way the same effect as a continuous cavity displacement from the low-pass filter is obtained at the second harmonic. When the oscillator is connected to a resistive load, the two-port $(A-A')-(B-B')$ becomes dissipative [28], [29], [30] and the above considerations no longer apply. However, experimental measurements performed as described in [24] on a scaled S-band mounting model show significant second harmonic impedance variations even when a post coupled oscillator is connected to a broad-band matched load. These results suggest that the proposed mount is suitable for the most extensive operating conditions. In the case of purely reactive loads at the second harmonic (i.e., filter), possible sharp resonances at this frequency can also be eliminated by simply varying d_c. Computer simulation performed following Joshii and Cornik theory [29] also demonstrates such a possibility (in the calculations the coupling to the cylindrical cavity, $(B-B')$ port in Figs. 5 and 6, was approximated by a gap in the post without the diode). The mounting described was then adjusted for varactor diode operations (Fig. 4(b)) and electronic tuning bands 40-percent wider than those for the same size mounting in Fig. 1(c), (a,b,c,s), were obtained.

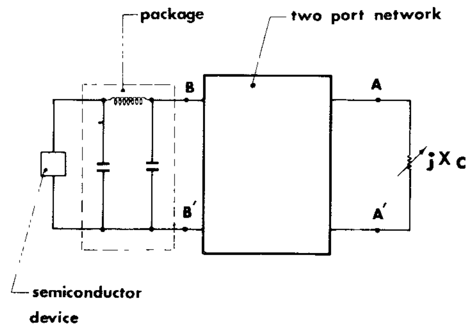

Fig. 5. An equivalent circuit of the mounting in Fig. 4.

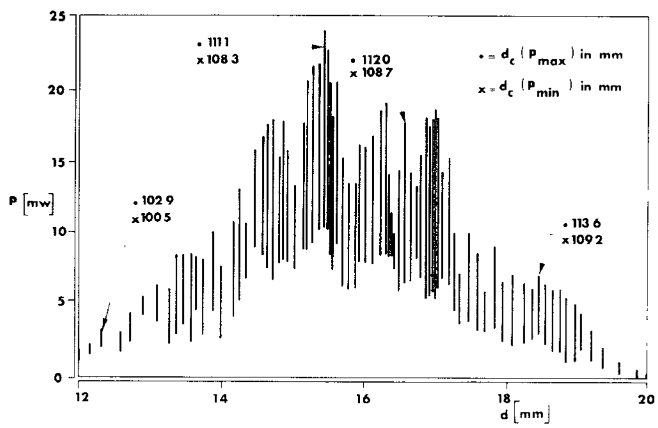

Fig. 6. Output power variations of a post-coupled oscillator obtained by varying the harmonic cavity short-circuit position (d_c). The results shown are for various fundamental frequency short-circuit tuning positions (d). Because $d_c \geqslant 10$ cm, the values corresponding to the maximum and minimum power varies rapidly with d and an interpolating curve cannot be easily drawn, so only some d_c values are reported here.

V. Experimental Results Obtained by Means of the New Mount

A. Output Power

A configuration with an iris and dielectric tuning rod was analyzed first. For each fundamental tuning condition power variations of 5–7 dB were observed when the harmonic cavity plunger position d_c was varied. The situation, for instance, was no different when a post coupled configuration reactively loaded at the harmonic frequencies was used (see the results in Fig. 6). When this oscillator was connected to a broad-band absorber, power variations of about 2 dB were obtained. The power P shows a periodic trend with d_c. The period corresponds to half the wavelength of the second harmonic signal in the circular waveguide TE_{11} mode [22].

B. Bias Tuning

Fig. 7 shows the effect of the harmonic tuning (d_c) on the $(f-V_d)$ and $(P-V_d)$ curves of an iris coupled oscillator. A really drastic linearization effect can be achieved for both type of diagrams. We can see that the power curves overlap close to the same V_d values as the frequency curves. Results of the same type were also obtained by using an oscillator without iris connected to the harmonic filter. Similar effects were noticed in the case of a frequency-modulated oscillator when we observed the curve of the modulation depth as a function of the RF voltage applied to the diode obtained with the Bessel function method.

C. Varactor Tuning

In Fig. 8, which shows the $(f-V_v)$ and $(P-V_v)$ curves for an iris-coupled oscillator, a drastic linearization effect in the $(f-V_v)$ curves can be observed (the maximum linearity deviation decreases from 8 percent to 0.5 percent). Moreover, as was to be expected, a smaller df/dV_v is obtained the more P increases with V_v (and therefore with f) at the operating point. Similar results were also obtained by using a post coupled configuration. In particular, it was noticed that very strong linearization effects cannot be obtained when the oscillator and the cylindrical cavity are connected to broad-band absorbers. In this case the computer simulation [29] shows a very flat second harmonic impedance trend. This proves that the nonlinearities of the frequency pulling phenomena can be ex-

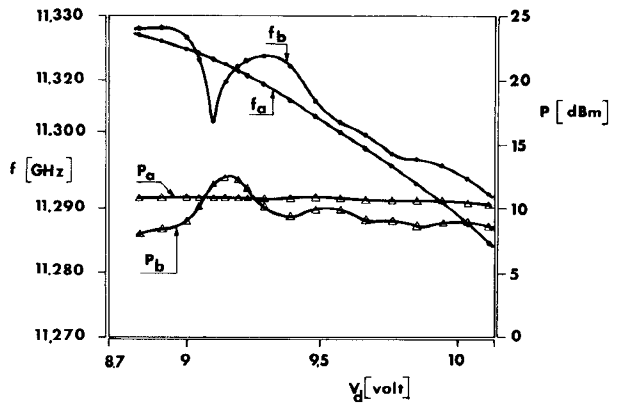

Fig. 7. Frequency (dots) and power (triangles) versus the diode bias voltage V_d for two different harmonic tuning short-circuit positions of an iris-coupled oscillator. ($d_c = 103.1$ mm for a curve and $d_c = 100.2$ mm for b curve).

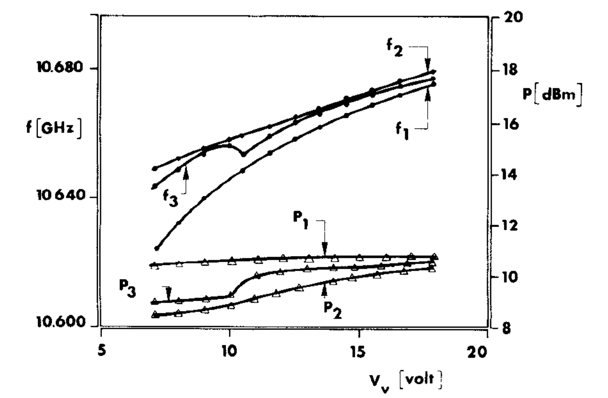

Fig. 8. Frequency f (dots) and power p (triangles) of an iris-coupled oscillator as functions of the varactor voltage V_v for three different harmonic tuning conditions ($d = 113.1$, $= 108.8$, $= 115.2$ mm for 1, 2, 3 curves, respectively). For $V_v = 14$ V, was $d_c(P_{max}) = 114.2$ mm and $d_c(P_{min}) = 109.8$ mm. The results reported in Fig. 7 for $d = 18.4$ mm refer to a post-coupled oscillator working at 10.64 GHz.

ploited in order to minimize the effects of the nonlinearity intrinsic to the modulating mechanism itself (e.g., the tuning with the varactor diode, whose capacitance varies as $1/\sqrt{V_v}$).

D. *Temperature Stability of the Operating Frequency*

Thermal variations affect both diode and cavity parameters. Talwar and Curtice [31] analyzed the temperature dependence of the diode impedance. Hobson and Desa [32] pointed out that for high V_d the bias tuning is mainly due to thermal effects. Both the bias tuning experiments (with only the diode parameters varied) and the varactor tuning experiments (with only the circuit load parameters varied) demonstrated strong dependence on the harmonic load conditions. It is therefore reasonable to expect a nonnegligible harmonic load effect on the temperature stability of the oscillator operating frequency. Such an effect was verified by recording the oscillator frequency f and the output power P as functions of the temperature T of an iris-loaded oscillator for several harmonic tuning

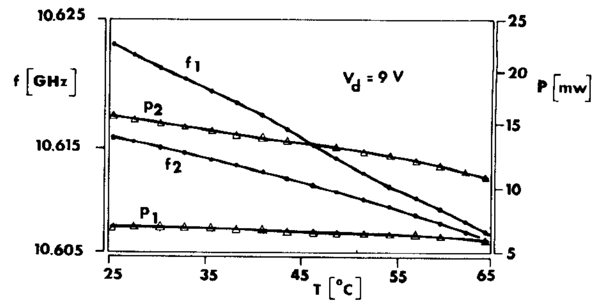

Fig. 9. Frequency (dots) and power (triangles) as functions of the temperature for two different harmonic tuning conditions for an iris-coupled oscillator. d_c see text.

short-circuit positions d_c. Under our operating conditions the frequency variation due to cavity thermal expansion was of the same order of magnitude as that due to thermal variations of the diode parameters. Fig. 9 shows the (f–T) curves obtained respectively for $d_c = 10.9$ cm (curve 1) and $d_c = 11.3$ cm (curve 2). Curve 1 shows an average value of $|df/dT|$ which seems to be even a little lower than the absolute value of the measured temperature derivative of the passive cavity resonance frequency. In any event, there is complete compensation for the variation effect of the diode parameters. It should be pointed out that it is not necessary to have a high-Q cavity in order to achieve this result (in fact, for thermal experiments, a relatively low-Q cavity was chosen, as is shown by the fact that the frequency drift due to the diode—fully removed by harmonic tuning—was of about the same magnitude as the thermal variation of the passive cavity resonance frequency). A preliminary test with a low-Q Invar cavity shows the possibility of obtaining frequency drift about one order smaller. Thermal compensation is difficult in relatively low-Q cavities such as those for pulsed operation, owing to drift variations from one diode to another. For instance, when cavities with metallized perspex walls are used [33], the perspex wall thickness must be different for each diode. Compensation with a thermal sensitive rod inserted into the cavity requires troublesome calibrations and is limited by the nonlinearity of frequency variations with temperature [33] especially when diodes with highly differing thermal drift are involved. For this reason, some designers prefer to stabilize the temperature instead of compensating their low-Q cavities. Fig. 9 shows that harmonic tuning makes it possible to vary the sensitivity of the noncompensated oscillator continuously between 450 and 250 kHz/°C. Now let us suppose that we compensate this cavity by using metallized perspex walls, thus varying the resonant frequency thermal drift by −350 kHz/°C. In this way with harmonic tuning it is possible to eliminate frequency drift differences, due to the spread, of $\sim\pm 100$ kHz/°C from diode to diode. This can be done simply by bringing the frequency, by means of harmonic tuning at low temperatures, back to the same value that was fixed by fundamental tuning at high temperatures. For mass production it thus seems possible to utilize only one kind of low-Q cavity, making the diode spread correction by harmonic tuning and eliminating the need for insertion of dielectrics of different thicknesses or for complicated calibration. When compensation rods are used, harmonic tuning seems useful to obtain broader stability ranges, since at low temperatures it corrects the overcompensation effect inherent in this system. Moreover, the possibility of employing fixed rough compensation allows the use of a standard low cost ceramic capacitance mounted directly on the diode [34], instead of a capacitance which would have to be calibrated for each separate diode.

E. FM Noise

With the change in the harmonic load circuit, the oscillator FM noise to signal ratio showed several dB variations. However, outstanding correlation between maximum FM noise and the $(f_{\max}, P_{\min})$ condition did not occur. This may be a consequence of the fact that at the operating point the factor $\delta a/\delta B_{0d}$ is strongly dependent on the spectral fluctuations of the upper harmonics. These fluctuations may affect the noise, even if they do not give rise to easily detectable pulling or output power effects. The structure described is therefore capable of reducing FM noise but the condition optimizing all the other performances may not coincide with the one providing the minimum FM noise to signal ratio.

VI. Conclusions

The output power, electronic tuning characteristics, FM noise and temperature stability of waveguide Gunn oscillators depend to a great extent on the harmonic frequency loads. Theoretical and experimental analyses of such effects are given with the aim of identifying useful design features. It is shown that simple practical oscillator cavities of various types can be easily constructed, which allow considerable improvement in all the performances mentioned by independent tuning of the fundamental and second harmonic signals over a very broad operating frequency range. It is proved that the frequency thermal stability and the FM–AFC oscillator characteristics are optimized when the harmonics are tuned to give the maximum output power level. Moreover, for varactor-tuned cavities, very strong reductions are obtained of intermodulation effects, due to nonlinear frequency dependence on the varactor voltage. The FM noise to signal ratio can be reduced by several decibels, although it cannot usually be optimized together with all the other performances. It is finally shown that harmonic tuning provides a simple means to continuously vary the magnitude of thermal drift of the oscillator operating frequency. This can simplify the design of temperature compensated low-Q oscillators.

Acknowledgment

The author wishes to thank Prof. F. J. Rosenbaum for his very helpful comments and valuable suggestions on this manuscript.

References

[1] I. W. Pence and P. J. Khan, "Broad-band equivalent-circuit determination of Gunn diode," *IEEE Trans. Microwave Theory Tech.*, vol. MTT-18, pp. 784–790, 1970.

[2] R. L. Eisenhart and P. J. Khan, "Some tuning characteristics and oscillation conditions of a waveguide-mounted transferred electron diode oscillator," *IEEE Trans. Electron Devices*, vol. ED-19, pp. 1050–1055, Sept. 1972.

[3] C. P. Jethava and R. L. Gunsor, "An analytical equivalent circuit representation for waveguide-mounted Gunn oscillators," *IEEE Trans. Microwave Theory Tech.*, vol. MTT-20, pp. 565–572, Sept. 1972.

[4] W. R. Curtice, "Quenched-domain mode oscillation in waveguide-circuits," *IEEE Trans. Microwave Theory Tech.*, vol. MTT-21, pp. 369–374, June 1973.

[5] M. J. Howes, "Circuit considerations in the design of wide-band tunable transferred-electron oscillators," *IEEE Trans. Electron Devices*, vol. ED-17, pp. 1060–1067, Dec. 1970.

[6] E. M. Bastida and G. Conciauro, "Influence of the harmonics on the power generated by waveguide tunable Gunn oscillators," *IEEE Trans. Microwave Theory Tech.*, vol. MTT-22, pp. 796–798, Aug. 1974.

[7] J. E. Carrol, "Resonant-circuit operation of Gunn-diodes. A self-pumped parametric oscillator," *Electron. Lett.*, vol. 2, pp. 215–216, 1966.

[8] M. E. Levinstein, L. S. Puscharoeva and M. S. Shur: "Influence of the second harmonic of a resonator on the parameters of a Gunn generator for transit and hybrid modes," *Electron. Lett.*, vol. 8, pp. 31–33, 1972.

[9] W. Frey, "Influence of a second harmonic voltage component on the operation of a Gunn oscillator," *Proc. MOGA Conf.*, (Amsterdam, The Netherlands), 1970.

[10] W. C. Tsai, F. J. Rosenbaum and L. A. Mackenzie, "Circuit analysis of waveguide cavity Gunn-effect oscillator," *IEEE Trans. Microwave Theory Tech.*, vol. MTT-18, pp. 808–817, 1970.

[11] G. King and H. P. Wasse, "Frequency modulation of a Gunn oscillator," *IEEE Trans. Electron Devices.*, vol. ED-14, pp. 717–718, Oct. 1967.

[12] W. C. Tsai and F. J. Rosenbaum, "Amplitude and frequency modulation of a waveguide cavity CW Gunn oscillator," *IEEE Trans. Microwave Theory Tech.*, vol. MTT-18, pp. 877–894, 1970.

[13] J. J. Stickler, "Injection-locking of Gunn oscillators with feedback stabilization," *Proc. IEEE*, vol. 157, pp. 1772–1773, 1969.

[14] D. Tang, R. J. Lomax and G. I. Haddad, "Effect of circuit load on the phase of bias-tuning in transferred electron devices," *Electron. Lett.*, vol. 9, pp. 564–565, 1973.

[15] E. M. Bastida, "Harmonic effects on the bias-tuning features of waveguide Gunn-diode oscillators," *Alta Freq.*, vol. 14, pp. 358–361, 1976.

[16] J. P. Quine, "A generalized locking equation for oscillators," *IEEE Trans. Microwave Theory Tech.*, vol. MTT-20, pp. 418–420, June 1972.

[17] E. M. Bastida *et al.*, "Indirect electron drift velocity versus electric field measurement in GaAs," *Appl. Phys. Lett.*, vol 18, pp. 28–31, 1971.

[18] E. M. Bastida, G. Conciauro, and G. Pierini, "A general program for the simulation of Gunn diode microwave oscillators," *Alta Freq.*, vol. 43, pp. 407–417, 1974.

[19] R. A. Kiehl and R. L. Gunshor, "Internal dynamics and microwave properties of X-band transferred electron devices," *IEEE Trans. Microwave Theory Tech.*, vol. MTT-24, pp. 165–171, Apr. 1976.

[20] Y. S. Wu, "Second harmonic characteristics of waveguide cavity CW Gunn oscillators," Thesis, Sever Inst. Washington Univ., St. Louis, MO, 1970.

[21] G. G. Endersz, "Linearity improvement of microwave FM oscillators by harmonic tuning," *IEEE Trans. Microwave Theory Tech.*, vol. MTT-23, pp. 360–367, Apr. 1975.

[22] H. Pollmann *et al.*, "Load dependence of Gunn oscillator performances," *IEEE Trans. Microwave Theory Tech.*, vol. MTT-18, pp. 817–827, 1970.

[23] J. G. Ruch and W. Fawcett, "Temperature dependence of the transport properties of Gallium Arsenide determined by a Monte Carlo method," *J. Appl. Phys.*, vol. 41, pp. 3843–3849, 1970.

[24] R. L. Eisenhart and P. J. Khan, "Theoretical and experimental

analysis of a waveguide mounting structure," *IEEE Trans. Microwave Theory Tech.*, vol. MTT-19, pp. 706–719, Aug. 1971.
[25] R. P. Owens and D. Cawsey, "Microwave equivalent circuit parameter of Gunn effect devices packages," *IEEE Trans. Microwave Theory Tech.*, vol. MTT-18, pp. 780–798, 1970.
[26] K. Wilson, "Gunn effect devices and their applications," *Mullard Techn. Comm.* vol. 10, pp. 286–293, 1969.
[27] A. A. Sweet and L. A. MacKenzie, "The FM noise of a C.W. Gunn oscillator," *Proc. IEEE* vol. 58, pp. 822–823, 1970.
[28] O. L. El-Sayed, "Generalized analysis of parallel two-post mounting structures in waveguide," *IEEE Trans. Microwave Theory Tech.*, vol. MTT-25, pp. 24–33, 1977.
[29] J. S. Joshi and A. F. Cornick, "Analysis of waveguide post configurations: part I—Gap admittance matrices," *IEEE Trans. Microwave Theory Tech.*, vol. MTT-25, pp. 169–173, Mar. 1977.
[30] ——, "Analysis of waveguide post configuration: part II—Dual gap cases," *IEEE Trans. Microwave Theory Tech.*, vol. MTT-25, pp. 173–181, Mar. 1977.
[31] K. Talwar, W. R. Curtice, "Effect of donor density and temperature on the performance of stabilized transferred-electron devices," *IEEE Trans. Electron. Devices*, vol. ED-20, pp. 544–550, June 1973.
[32] G. S. Hobson and B. A. E. DeSa, "Thermal effects in the bias circuit frequency modulation of Gunn oscillators," *IEEE Trans. Electron. Devices*, vol. ED-18, pp. 557–562, 1971.
[33] R. Stevens and F. A. Myers, "Temperature compensation of Gunn oscillator," *Electron. Lett.*, vol. 10, pp. 461–463, 1974.
[34] A. Kondo, T. Ishii and K. Shirata, "Simple stabilizing method for solid state microwave oscillators," *IEEE Trans. Microwave Theory Tech.*, vol. MTT-22, pp. 970–972, Nov. 1974.

Theory and Simulation of the Gyrotron Traveling Wave Amplifier Operating at Cyclotron Harmonics

KWO RAY CHU, ADAM T. DROBOT, HAROLD HWALING SZU, and PHILLIP SPRANGLE

***Abstract*—An analytical expression for the efficiency of the gyrotron traveling wave amplifier is derived for the case of nonfundamental cyclotron harmonic interaction. It scales the efficiency with respect to the modes and parameters of operation. This relation, together with a general linear dispersion relation, also derived in the present paper, gives the characteristics and optimum operation conditions of the gyrotron traveling wave amplifier.**

I. Introduction

AN INTERESTING electromagnetic radiation mechanism [1]–[3] known as the electron cyclotron maser has been the subject of intense research activities in recent years. This mechanism has been the basis for a new class of microwave devices called gyrotrons capable of generating microwaves at unprecedented power levels at millimeter and submillimeter wavelengths. A detailed description of the cyclotron maser mechanism is given in [4] and brief summaries of gyrotron theories and experiments, together with lists of references, can be found in recent review papers [5]–[7].

In the present study, we will concentrate on a particular type of gyrotrons—the gyrotron traveling wave amplifier (gyro-TWA). The cyclotron maser instability and its wide-band amplification capability was demonstrated experimentally by Granatstein *et al.* [8] on an intense relativistic electron beam. The basic physical processes taking place in a gyro-TWA have been analyzed in recent linear and nonlinear theories [4], [9]–[16]. In the actual operation of a gyro-TWA, the beam-to-wave energy conversion efficiency is one of the most important considerations. References [12]–[14] contain detailed studies of the saturation mechanisms and calculations of efficiency for the operation at the fundamental cyclotron harmonic. However, the scaling of the efficiency with respect to the various modes and parameters of operation has not been considered in any detail, nor has the operation at the nonfundamental cyclotron harmonics. The nonfundamental harmonic operation is of great importance for the amplification of submillimeter waves if unrealistically high magnetic fields (> 100 kG) are to be avoided. In anticipation of the growing experimental effort aimed at the generation of submillimeter waves, our main purpose in the present study is to derive a general analytical expression for the operating efficiency.

Manuscript received May 30, 1979; revised November 26, 1979. This work was supported by Rome Air Development Center under MIPR FY761970026.

K. R. Chu, H. H. Szu, and P. Sprangle are with the Naval Research Laboratory, Washington, DC 20375.
A. T. Drobot is with Science Applications, Inc., McLean, VA 22101.

II. Derivation of a General Dispersion Relation

The typical configuration of a gyro-TWA consists of an annular electron beam propagating inside a waveguide of

0018-9480/80/0400-0313$00.75 ©1980 IEEE